Journal of Photochemistry & Photobiology, B: Biology 189 (2018) 193–200

Contents lists available at ScienceDirect

Journal of Photochemistry & Photobiology, B: Biology

journal homepage: www.elsevier.com/locate/jphotobiol

Irradiation by ultraviolet light-emitting diodes inactivates influenza a viruses by inhibiting replication and transcription of viral RNA in host cells

Risa Nishisaka-Nonaka[a,1], Kazuaki Mawatari[a,*,1], Tomomi Yamamoto[a], Mizuki Kojima[a], Takaaki Shimohata[a], Takashi Uebanso[a], Mutsumi Nakahashi[b], Takahiro Emoto[c], Masatake Akutagawa[c], Yohsuke Kinouchi[c], Takahiro Wada[d], Masayuki Okamoto[d], Hiroshi Ito[d], Ken-ichi Yoshida[d], Tomo Daidoji[e], Takaaki Nakaya[e], Akira Takahashi[a]

[a] Department of Preventive Environment and Nutrition, Institute of Biomedical Sciences, Tokushima University Graduate School, Kuramoto-cho 3-18-15, Tokushima City, Tokushima 770-8503, Japan
[b] Graduate School of Bioscience and Bioindustry, Tokushima University, Minamijyousanjima-cho 2-1, Tokushima City, Tokushima 770-8506, Japan
[c] Graduate School of Science and Technology, Tokushima University, Minamijyousanjima-cho 2-1, Tokushima City, Tokushima 770-8506, Japan
[d] Nihon Funen Co., Ltd, 179-1 Mitsujima-shinden, Kawashima-cho, Yoshinogawa City, Tokushima 779-3394, Japan
[e] Department of Infectious Diseases, Graduate School of Medical Science, Kyoto Prefectural University of Medicine, 465 Kajii-cho, Kawaramachi-Hirokoji, Kamigyo-ku, Kyoto 602-8566, Japan

A B S T R A C T

Influenza A viruses (IAVs) pose a serious global threat to humans and their livestock, especially poultry and pigs. This study aimed to investigate how to inactivate IAVs by using different ultraviolet-light-emitting diodes (UV-LEDs). We developed sterilization equipment with light-emitting diodes (LEDs) those peak wavelengths were 365 nm (UVA-LED), 310 nm (UVB-LED), and 280 nm (UVC-LED). These UV-LED irradiations decreased dose fluence-dependent plaque-forming units of IAV H1N1 subtype (A/Puerto Rico/8/1934) infected Madin-Darby canine kidney (MDCK) cells, but the inactivation efficiency of UVA-LED was significantly lower than UVB- and UVC-LED. UV-LED irradiations did not alter hemagglutination titer, but decreased accumulation of intracellular total viral RNA in infected MDCK cells was observed. Additionally, UV-LED irradiations suppressed the accumulation of intracellular mRNA (messenger RNA), vRNA (viral RNA), and cRNA (complementary RNA), as measured by strand-specific RT-PCR. These results suggest that UV-LEDs inhibit host cell replication and transcription of viral RNA. Both UVB- and UVC-LED irradiation decreased focus-forming unit (FFU) of H5N1 subtype (A/Crow/Kyoto/53/2004), a highly pathogenic avian IAV (HPAI), in infected MDCK cells, and the amount of FFU were lower than the H1N1 subtype. From these results, it appears that IAVs may have different sensitivity among the subtypes, and UVB- and UVC-LED may be suitable for HPAI virus inactivation.

1. Introduction

Influenza viruses belong to the family *Orthomyxoviridae*. They contain a single-stranded negative-sense RNA genome comprising eight segments. The influenza viruses are classified as A, B, or C based on their core proteins. Influenza A viruses (IAVs) have two specific surface antigens: hemagglutinin (HA) and neuraminidase (NA) [1]. HA is the most abundant protein, forming a homotrimer structure on the viral surface. This structure mediates attachment to the host cell surface via binding to sialic acid (SA) residues of cellular receptors, triggering fusion of the viral envelope with the endosomal membrane, thereby releasing the viral genome into the cytoplasm [2]. NA cleaves glycosidic bonds with terminal SA, facilitating the release of budding virions from the cell [2]. Due to antigenic drift and shift, novel mutants of IAVs are frequently detected and can cross species barriers. Therefore, IAVs remain a serious global problem for humans and their livestock, especially poultry and pigs. Avian influenza (AI) viruses are classified by their pathogenic phenotype in chickens [3]. The critical genetic difference determining a low pathogenic (LPAI) or the highly pathogenic (HPAI) phenotype depends on the HA cleavage site [4]. HPAI viruses, such as H5N1 and H7N9, have only two HA subtypes: H5 and H7 [4]. From January to March 2004, HPAI virus H5N1 subtype infected chickens at four poultry farms in Oita, Yamaguchi, and Kyoto Prefectures, Japan, in an acute, lethal, and highly transmissible outbreak [5]. H5N1 subtypes emerged as a human pathogen in 1997 with the expected potential to undergo sustained human-to-human transmission and pandemic viral spread [6]. From 2003 to 2016, World Health Organization (WHO) reported > 850 individuals infected by the H5N1 subtype in > 12 countries with clinical mortality > 50% [7]. Therefore, H5N1 subtypes can cause serious public health problems in birds and

* Corresponding author.
E-mail address: mawatari@tokushima-u.ac.jp (K. Mawatari).
[1] Risa Nishisaka-Nonaka and Kazuaki Mawatari contributed equally to this work.

https://doi.org/10.1016/j.jphotobiol.2018.10.017
Received 14 June 2018; Received in revised form 11 October 2018; Accepted 18 October 2018
Available online 29 October 2018
1011-1344/

humans and are one of the most infectious avian diseases transmissible to humans. Further effective strategies are urgently required to prevent HPAI virus infection.

The viral contamination of water has long been suspected a major factor in the persistence and spread of HPAI H5N1 infection to chickens. Wild waterfowl are considered the reservoir for both LPAI and HPAI viruses. Lakes and rivers are important migratory bird breeding sites and have experienced several HPAI epizootics. Water-borne river transmission could have partly contributed to the spread of HPAI H5N1 during the 2004 Thailand epidemic [8]. In the Qinghai Lake region of China, AI virus H9N2 subtype was isolated from plateau pikas (*Ochotona curzoniae*) from November 2008 to October 2009 [9]. These reports suggest that disinfection of drinking water from rivers and lakes is essential to prevent AI virus transmission to humans and chickens, especially in poultry farms. To prevent AI virus infections, chlorination has high efficiency against viruses in general. However, some health problems have been observed. For instance, residual chlorine in drinking water can cause the formation of potentially carcinogenic halogenated by-products [10]. Other methods of disinfection include sunlight or ultraviolet (UV) irradiation, which produces by-products but these reported so far are below the level of health concerns [11]. The majority UV disinfection systems currently utilize low- or medium-pressure mercury lamps, which are toxic, require significant amounts of energy, and have a short lifespan. Furthermore, mercury is acutely toxic and is a major persistent environmental pollutant [12,13]. Instead of mercury lamps, UV light-emitting diodes (UV-LEDs) have recently been developed as an alternative UV light emission source, providing highly energy-efficient, reliable, and simple generation of near UV light. UV-LEDs do not contain toxic elements that could be released upon breakage and have a much longer lifespan. Given their small size, multiple diodes can emit different peak wavelengths into unique designed reactor [14].

UV rays are classified by wavelength into UVA (320–400 nm), UVB (280–320 nm), and UVC (100–280 nm). Low-pressure UV lamps (LPUV) can radiate a monochromatic peak wavelength (254 nm) and are utilized in the common water treatment processes of removing and inactivating viral and microbial pathogens by damaging their genome [15]. While mercury lamps only emit light at one wavelength or over a broad wavelength range, UV-LEDs are capable of emitting light at multiple individual wavelengths [16]. LEDs are created by connecting p- and n-type semiconductors that move electrons into positively charged holes between the two materials. The light wavelength depends on the type of material used for the two semiconductors. Indium gallium nitride (InGaN) is a widely available semiconductor for high-efficiency blue light or UVA ranges, initially innovated by Dr. Shuji Nakamura (University of California, Santa Barbara, USA) and colleagues, who received the Nobel Prize in Physics, 2014. InGaN-based UVA-LEDs can demonstrate near 50% external quantum efficiencies, but cannot radiate a deep UV wavelength. Recently, aluminum gallium nitride (AlGaN) has been used as a semiconductor for deeper a UV range (250–350 nm) and has been manufactured for many potential applications, including microbial disinfection. However, the external quantum efficiencies of AlGaN-based UV-LEDs remain < 2%, even for the best devices.

In this study, we irradiated IAV virus suspensions utilizing three UV-LEDs with peak wavelengths of 365, 310, and 280 nm, respectively. The reports about inactivation effects of UV-LED irradiations on microorganism are increasing in recent years [17–20]. UV-LED at different peak wavelengths (265, 280, 310, and 365 nm) had inactivation effect on *E. coli* [14,17,18]. Rattanakul S et al. and Beck SE et al. compared the inactivation effect among different UV-LEDs and LPUV on not only gram-negative bacteria but gram-positive bacteria, bacteriophage, and human adenovirus [19,20]. However there are few studies about the effect of UV-LED irradiation on IAVs. Our previous studies have reported that an originally developed UVA-LED (365 nm) irradiating system could inactivate enteropathogenic bacteria, MS2 phages, and *Cryptosporidium parvum* oocysts [21,22]. UVA-LED irradiation induces cellular membrane damage and delays growth indirectly by increasing levels of reactive oxygen species, including superoxide anion radicals (O_2^-), hydroxyl radicals (OH^-), hydrogen peroxide (H_2O_2), and singlet oxygen ($^1O_2$) [21]. However, it remains unknown whether UVA-LED irradiation can inactivate IAVs. Irradiation from UVB- and UVC-lamps had an inactivating effect on the infectivity of two HPAI viruses, one of which was the H5N1 subtype [23,24]. However, these mechanisms of HPAI virus inactivation remain unclear. The aims of this study were: (1) to compare the efficiencies of viral inactivation of IAV by different UV-LED irradiations, (2) to investigate how to inactivate IAV by different UV-LED irradiations, and (3) to compare the sensitivity of different IAV subtypes, including HPAI virus to UV-LED irradiation.

2. Materials and Methods

2.1. Cells and Virus Strains

Madin-Darby canine kidney (MDCK) cells and an IAV H1N1 subtype (strain A/Puerto Rico/8/1934) were kindly gifted by Prof. Akio Adachi (Tokushima University Graduate School). An HPAI H5N1 subtype (strain A/crow/Kyoto/53/2004) was obtained from Research Foundation for Microbial Diseases, Osaka University. MDCK cells were cultured at 37 °C, 5% CO_2, in Dulbecco's modified Eagle's medium (DMEM) supplemented with 5% fetal bovine serum (AusGeneX, Oxenford, Australia) and 60 μg/mL kanamycin (WAKO Pure Chemical Industries, Ltd., Tokyo, Japan). The virus suspension was prepared for irradiation experiments by propagating the IAV subtypes in 10-day-old embryonated eggs (Ishii Poultry Agricultural Cooperative, Tokushima, Japan) for 48 h at 37 °C. All experiments using the H5N1 subtype were performed in a Biosafety Level 3 laboratory at the Kyoto Prefectural University of Medicine.

2.2. UV-LEDs and Irradiation of the Virus Suspension

Three different peak wavelength UV-LEDs (Nichia, Tokushima, Japan) were used to irradiate the viral suspensions in this study. A volume of 0.3 mL virus suspension, with an infectivity titer of 0.3–1.1 × 10^6 plaque-forming units (PFU)/mL or 2.3–4.0 × 10^6 focus-forming units (FFU)/mL, was placed in a stainless steel cylinder cup (10 mm diameter and depth). The UV wavelengths were emitted downward onto the surface of the solution. The peak wavelengths of each diode were 365 nm (UVA-LED, NC4U134A), 310 nm (UVB-LED, NCSU234A), and 280 nm (UVC-LED, NCSU234A). The UV-LED irradiation systems were originally developed in this study (Fig. 1). The three individual LEDs were on a printed circuit board (Audio-Q, Shizuoka, Japan, Fig. 1a) and connected in series to a current-controlling single power source (PAS40-9, Kikusui Electronics Corp., Kanagawa, Japan). These diodes irradiated the viral suspension under maximum forward current (IF) according to the manufacturer's instructions and the fluence rates were 106 mW/cm^2/s (IF = 0.6 A, 365 nm) 4.4 mW/cm^2/s (0.35 A, 310 nm), and 5.5 mW/cm^2/s (0.35 A, 280 nm) (Fig. 1b and c). The UV spectral fluence rates (mW/cm^2/s/nm) on the surface of samples were measured six times during UV-LED irradiation using an MCPD 3700A multiple wavelength photometer (Otsuka Electronics, Osaka, Japan). The fluence rates were calculated by the sum of averaged spectral fluence rates between 200 nm and 400 nm.

2.3. Plaque-Forming Assay

A plaque-forming assay was performed in MDCK cells to determine the PFU so that the infectivity titer could be calculated. After UV irradiation of the virus suspensions, MDCK cells cultured in 6-well plates with DMEM were infected with 10-fold serial dilutions of the virus suspensions and incubated at 37 °C for 1 h. An unirradiated virus suspension was used as a dark control. After removing these virus

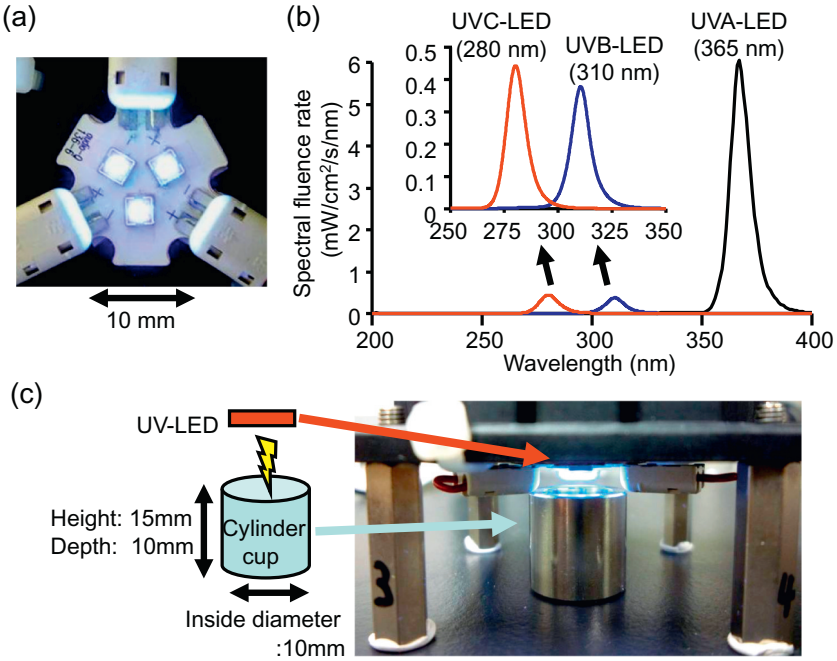

Fig. 1. Emission spectrum and system setup of UV-LEDs used in this study. (a) Photograph of UV-LEDs. (b) Emission spectrum of UV-LEDs. (c) Schematics and photograph of UV-LED irradiation system setup.

suspensions, DMEM containing 1.1% agar and 2 μg/mL trypsin was added to the cells as an overlay (Thermo Fisher Scientific, Waltham, MA, USA). Following 48 h incubation, the cells were stained with 0.5% crystal violet solution containing 10% formalin for PFU counting. The effects on viral activation caused by the LED irradiations were assessed using the log PFU ratio, which was calculated as log PFU ratio = $\log_{10}$ (*Nt/N0*), where *Nt* is the PFU count of the UV-irradiated sample, and *N0* is the PFU count of the sample without UV irradiation.

2.4. Focus-Forming Assay

MDCK cells were cultured in 48-well plates. At 13 h post-infection with UV-irradiated virus suspensions, the cells were fixed for 30 min at room temperature with buffered 4% paraformaldehyde and washed three times with phosphate buffered saline (PBS). An unirradiated virus suspension was used as a control. Then, the cells were then stained with a rabbit polyclonal antibody against an LPAI virus H5N2 subtype (strain A/duck Hong Kong/342/1978) to detect influenza virus antigens. This antibody recognizes influenza virus NP and M1 proteins [25]. Antibody-binding viral proteins were detected with an Alexa Fluor 488-conjugated secondary antibody (Molecular Probes, Carlsbad, CA) diluted 1:500 in PBS containing 1% bovine serum albumin. An IX71N fluorescent microscope (Olympus, Tokyo, Japan) was used to observe the cells and count the FFUs. The effects of the LED irradiations on viral activation were determined by the infection ratio ($\log_{10}$) (log FFU ratio), which was calculated as log FFU ratio = $\log_{10}$ (*Nt/N0*), where *Nt* is the FFU count of the UV irradiated sample, and *N0* is the FFU count of the sample without UV irradiation.

2.5. Hemagglutination Assay

The hemagglutination (HA) titer of the virus suspension was measured using a standard HA assay [26]. Two-fold serial dilutions of virus suspensions with or without UV irradiation were applied to a round-bottomed 96-well plate and then mixed with 0.5% chicken red blood cells (Kohjin Bio Co., Ltd., Saitama, Japan). After incubation for 3 h at room temperature, the HA titers were determined as the highest dilution at which complete agglutination was observed.

2.6. RNA Extraction

To isolate total viral RNA from the viral suspension or infected MDCK cells, we used a QIAamp Viral RNA Mini Kit (Qiagen, CA, USA) according to the manufacturer's instructions. To isolate viral RNA from MDCK cells, we first irradiated the virus suspensions using the UV-LED. Then, MDCK cells in a 60 mm diameter culture dish with DMEM were infected with 10-fold dilutions of the virus suspension at 37 °C for 1 h. After removing these virus suspensions, DMEM containing 2 μg/mL trypsin was added to the cells. At 2, 4, 6, and 8 h post-infection, the cells were washed three times with ice-cold PBS, and total RNA was extracted and purified using an RNeasy Mini Kit (Qiagen) according to the manufacturer's instructions. RNA was quantified spectrophotometrically (Beckman Coulter, Brea, CA, USA).

2.7. Reverse Transcription

The expression levels of total RNA and three types of influenza virus RNA in the infected cells were measured by reverse transcription (RT)-quantitative real-time polymerase chain reaction (qPCR). The three types of RNA were mRNA (messenger RNA), vRNA (viral RNA), and cRNA (complementary RNA). vRNAs are genomic RNA, replicated via cRNAs to create progeny viruses. Viral mRNAs are transcribed for the translation of viral proteins [11]. For the measurement of total viral RNA, the RT reaction was performed with 500 ng purified RNA and both random hexamer and Oligo(dT) primers using a First Strand cDNA synthesis kit (TaKaRa Bio, Shiga, Japan). RT of the three types of influenza viral RNA was performed with tagged-primers (Table 1) using SuperScript™ III Reverse Transcriptase (Invitrogen), as described by Kawakami E et al. [27]. A 5.5 μL mixture containing approximately 200 ng total RNA and 10 ρmol of tagged primer was heated for 10 min at 65 °C and then immediately chilled on ice for 5 min. Next, 14.5 μL of preheated reaction mixture containing 4 μL First Strand Buffer, 1 μL 0.1 M dithiothreitol, 1 μL of 200 U/μL Superscript III reverse transcriptase (all Thermo Fisher Scientific); 4 μL dNTP mix, 10 mM each, (Takara Bio); 1 μL of 40 U/μL RNasin® Plus RNase Inhibitor (Promega, Fitchburg, WI, USA); and 3.5 μL saturated trehalose (WAKO Pure Chemical Industries, Ltd.), was added and incubated at 60 °C for 1 h.

Table 1
Characteristics of the primer sets for conventional and strand-specific RT-qPCR using tagged primers for quantification of the vRNA, cRNA, and mRNA of H1N1 segment 6.

Target	Purpose	Sequence (5′–3′)	Position (nt)
vRNA	RT	GGCCGTCATGGTGGCGAAT ACTATAATGACTGATGGCCCGAGT	693–716
	qPCR forward	GGCCGTCATGGTGGCGAAT	
	qPCR reverse	ACATCACTTTGCCGGTATCAGGGT	843–819
cRNA	RT	GCTAGCTTCAGCTAGGCATC AGTAGAAACAAGGAGTTTTTTGAAC	1413–1389
	qPCR forward	GCTAGCTTCAGCTAGGCATC	
	qPCR reverse	TGAATAGTGATACTGTAGATTGGTCT	1318–1343
mRNA	RT	CCAGATCGTTCGAGTCGT TTTTTTTTTTTTTTTTGAACAGACTAC	1398–1382
	qPCR forward	CCAGATCGTTCGAGTCGT	
	qPCR reverse	TGAATAGTGATACTGTAGATTGGTCT	1318–1343
Conventional	qPCR forward	CCGGCCATGGGTGTCTTTC	875–893
	qPCR reverse	TCCCTTTACTCCGTTTGCTCCATC	996–1019

Tagged sequences are in bold. RT, reverse transcription; qPCR, quantitative real time polymerase chain reaction; vRNA, viral RNA; cRNA, complementary RNA; mRNA, messenger RNA.

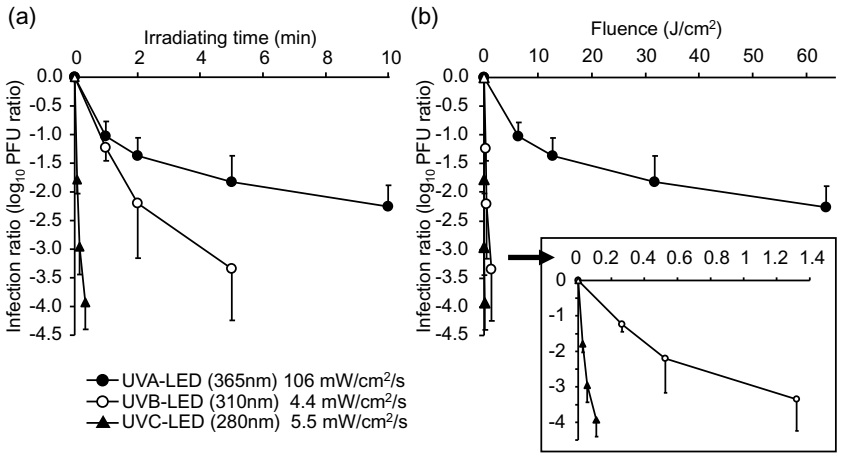

Fig. 2. Inactivation effect of UV-LED irradiations in influenza A virus H1N1 subtype. Viral suspensions of H1N1 subtype (strain A/Puerto Rico/8/1934) were infected into MDCK cells, which were irradiated using different peak wavelength UV-LEDs: UVA-LED (365 nm), UVB-LED (310 nm), and UVC-LED (280 nm). The viral inactivation effects of these LED irradiations were determined by the infection ratio (log_{10}), the ratio of plaque-forming units (PFUs), as described in the Materials and Methods section. Viral inactivation effects were dependent on irradiating time (a) and were fluence-dependent (b). Values are presented as means ± SD (n = 3–4, n = number of independent replicates).

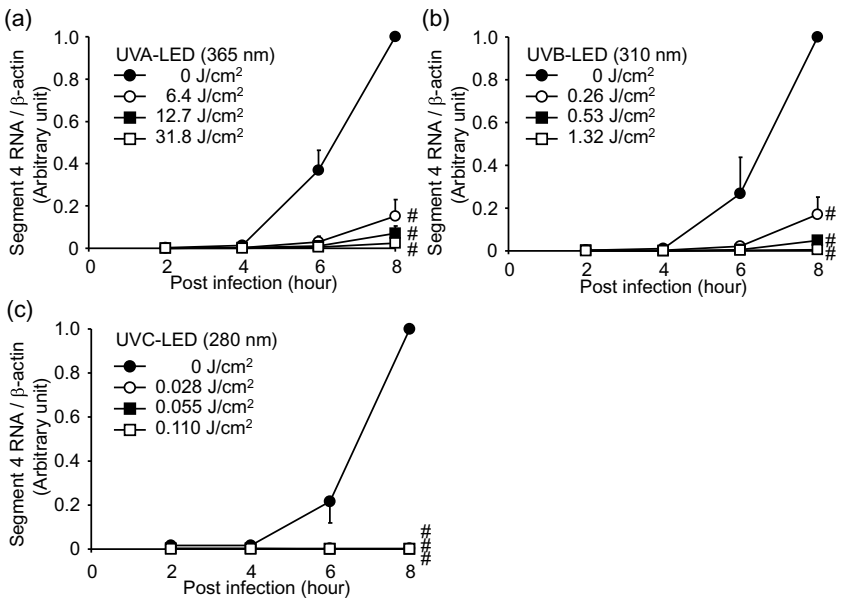

Fig. 3. Effect of UV-LED irradiations on total vRNA synthesis in host cells. MDCK cells were infected with viral suspensions of H1N1 subtype (strain A/Puerto Rico/8/1934) irradiated by UVA-LED (a), UVB-LED (b), or UVC-LED (c).s. Total viral RNA levels in the host cells were quantified by reverse transcription-quantitative real-polymerase chain reaction (RT-qPCR) with specific primers for segment 4, as described in the Materials and Methods section. β-actin was used as the internal control of host cellular RNA. Values are shown as means ± SD (n = 3, n = number of independent replicates). # indicates $P < 0.01$ for irradiation vs. non-irradiation.

2.8. Quantitative (Real-Time) PCR

Real-time PCR was performed with SYBR® Premix Ex Taq™ II (Takara Bio) using a LightCycler® 2.0 Real-Time PCR System (Roche, Mannheim, Germany). We added 1.2 µL cDNA to the qPCR reaction mixture containing 6 µL SYBR® Premix Ex Taq™ II, 0.24 µL forward primer (10 µM), 0.24 µL reverse primer (10 µM), and 4.32 µL double-distilled water. For qPCR, the reactions were heated at 95 °C for 30 s followed by 40 cycles of 10 s denaturing at 95 °C, 20 s annealing at 60 °C, and 15 s extension at 72 °C. The H1N1 subtype segment 4 primers, 5'-AATTTGCTATGGCTGACGGA-3′ (forward) and 5'-CTACAGAG ACATAAGCATTTTC-3′ (reverse), were used to quantify the total viral

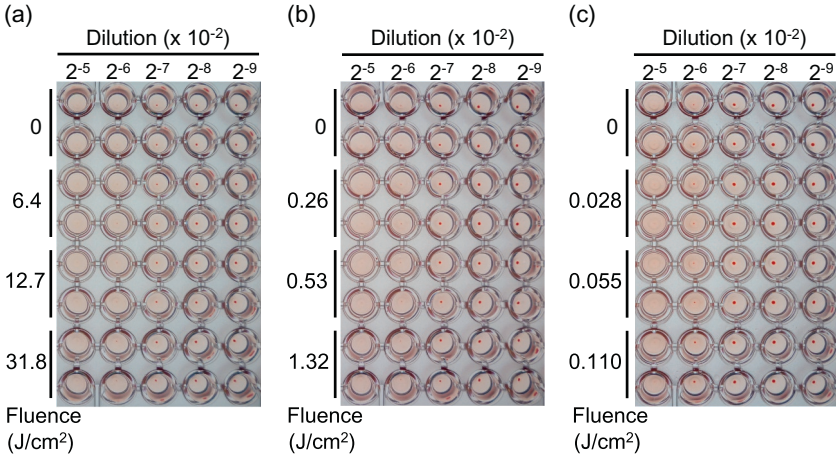

Fig. 4. Effect of UV-LED irradiation on the hemagglutination titer. Viral suspensions of H1N1 subtype (strain A/Puerto Rico/8/1934) were irradiated by UV-LEDs, and the hemagglutination activity was determined as described in the Materials and Methods section. (a) UVA-LED, (b) UVB-LED, and (c) UVC-LED irradiation.

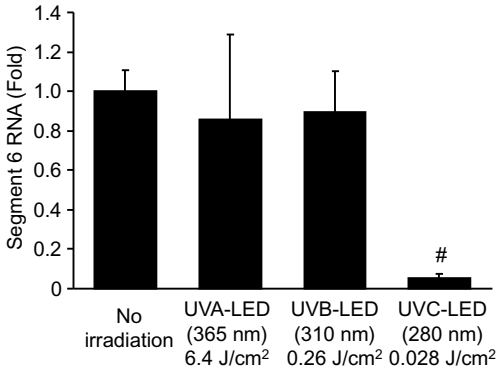

Fig. 5. Effect of UV-LED irradiation on vRNA. Viral suspensions of H1N1 subtype (strain A/Puerto Rico/8/1934) were irradiated at 6.4 J/cm^2 (UVA-LED), 0.26 J/cm^2 (UVB-LED), or 0.028 J/cm^2 (UVC-LED). The fluences of LED irradiations were capable of decreasing the PFU count of H1N1 subtype approximately 10-fold (log10 = −1) (Supplemental fig. S1). Viral RNA damage was measured by vRNA (segment 6) strand-specific RT-qPCR, as described in the Materials and Methods section. Results are displayed as means ± SE. # indicates $P < 0.01$ for irradiation vs. non-irradiation.

RNA. The primers for strand-specific qPCR of the H1N1 subtype segment 6 are listed in Table 1. The expression levels among the three types of viral RNA were compared using qPCR with conventional primers. The primers for β-actin, 5'-GACTACCTCATGAAGATCCTCACG-3′ (forward) and 5'-TCTCCTTGATGTCACGCACAATT-3′ (reverse), were used as internal controls for the host cellular RNA.

2.9. Statistical Analysis

Statistical analysis of differences was performed using ANOVA with Bonferroni's multiple comparison tests using Statview 5.0 software (SAS Institute Inc., Cary, NC, USA). Student's *t*-test was used for paired data where appropriate. $P < 0.05$ or $P < 0.01$ was considered statistically significant, according to the analysis performed.

3. Results

3.1. Inactivation Effects of Irradiations of Different UV-LEDs on IAV H1N1 Subtype

To determine the effects of different UV-LED irradiations on IAV, we prepared three UV-LEDs with peak wavelengths of 365 nm (UVA-LED), 310 nm (UVB-LED), and 280 nm (UVC-LED), and irradiated virus suspensions of H1N1 subtype (strain A/Puerto Rico/8/1934). MDCK cells were infected with the irradiated virus suspensions, and the inactivation effects were determined by comparison of the PFUs with a non-irradiated dark control (Fig. 2). UVA-LED irradiation decreased the PFUs 100-fold ($\log_{10} = -2$), but this required a higher fluence (63.6 J/cm^2) and longer irradiation time (10 min) than the other UV-LEDs. UVB- and UVC-LED irradiation decreased the PFUs > 1000-fold ($\log_{10} = -3$), and UVC-LED inactivated the virus at a lower fluence and a shorter irradiation time than UVB-LED. These results revealed that as the peak wavelength of UV-LED became shorter, the inactivation effect on the H1N1 subtype increased.

3.2. Effect of UV-LED Irradiations on Viral RNA Synthesis in MDCK Cells

To study the effect of different UV-LED irradiations on the growth of IAV in infected MDCK host cells, we performed RT-qPCR to quantify the total viral RNA. First, we synthesized cDNA from all RNA species using RT, and then we measured total viral RNA by quantitative real-time PCR (Fig. 3). The total viral RNA levels in the cells infected with non-irradiated virus suspension steadily increased 4 h post-infection. UVA- and UVB-LED irradiations suppressed the dose-dependent accumulation of total viral RNA in the infected cells. Additionally, UVC-LED irradiation completely inhibited viral growth. These results revealed that viral suspensions irradiated with UV-LEDs exhibited suppressed growth in host cells.

3.3. Effect of UV-LED Irradiations on Viral Hemagglutination Activity

To investigate the effect of different UV-LED irradiations on the binding capacity of IAV H1N1 subtype, we measured the hemagglutination activities of virus suspensions with and without UV-LED irradiation. UVA-, UVB-, and UVC-LED irradiation did not affect hemagglutination activities (Fig. 4), suggesting that UV-LED irradiations did not affect the binding capacity of IAV to host cells.

3.4. Effect of UV-LED Irradiation on Viral RNAs

To measure the viral RNA damage caused by LED irradiation, we purified viral RNA from strand-specific RT-qPCR of viral suspensions irradiated by UV-LEDs, as described in the Materials and Methods section. To equalize the inactivation effect, the UV-LED fluences were fixed at 6.4 J/cm^2 (UVA-LED), 0.26 J/cm^2 (UVB-LED), and 0.028 J/cm^2 (UVC-LED), respectively, being the amounts capable of an approximate 10-fold (log10 = −1) decrease in PFUs of the H1N1 subtype (Supplemental fig. S1). UVC-LED irradiation decreased the relative

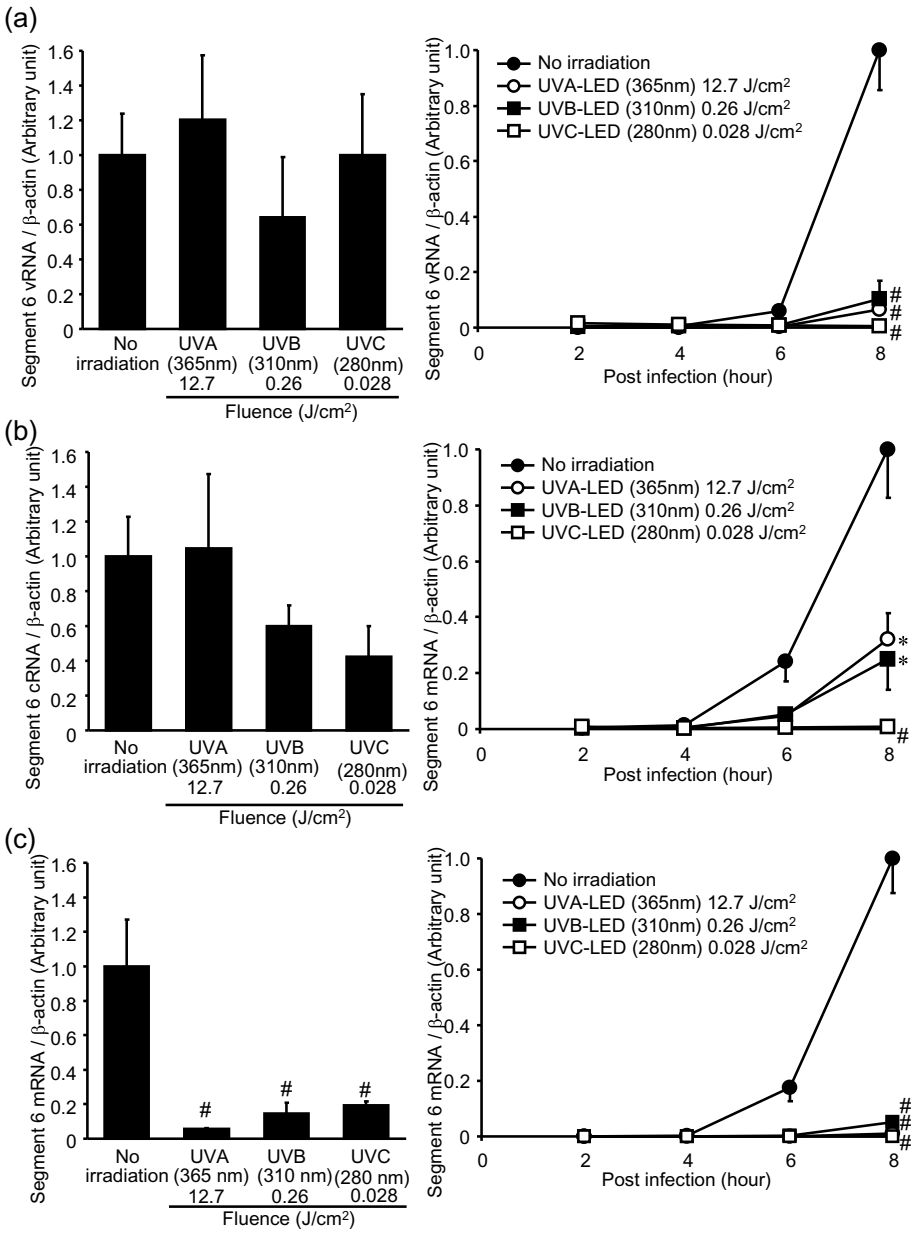

Fig. 6. Effects of UV-LED irradiations on the accumulation of three different strand types of viral RNA in the host cells: (a) vRNA, (b) cRNA, and (c) mRNA. Viral suspensions of H1N1 subtype (strain A/Puerto Rico/8/1934) were irradiated by 6.4 J/cm^2 (UVA-LED), 0.26 J/cm^2 (UVB-LED), or 0.028 J/cm^2 (UVC-LED), and infected into MDCK cells. The fluences of LED irradiations were capable of an approximate 10-fold PFU decrease (log10 = −1) of H1N1 subtype (Supplemental fig. S1). Three different strand types were Remark 12quantified by strand-specific RT-qPCR with tagged primers for segment 6, as described in the Materials and Methods section. The left panel only shows the RNA levels at 2 h post-infection. Values are displayed as means ± SE (n = 3–8, n = number of independent replicates). * indicates $P < 0.05$ and # indicates $P < 0.01$ for irradiation vs. non-irradiation.

level of viral RNA, but both UVB- and UVA-LED irradiation did not, suggesting that UVC-LED could damage viral RNA (Fig. 5).

3.5. Effect of UV-LED Irradiation on the Accumulation of Different Strand RNAs in MDCK Cells

To investigate the detailed effects of UV-LED irradiation on the accumulation of viral RNA in host MDCK cells, we observed the intracellular kinetics of different types of IAV RNA: viral RNA (vRNA), complementary RNA (cRNA), and messenger RNA (mRNA). To examine the effect of different UV-LED irradiations on the transcription and replication of viral RNA, we measured the three RNA species utilizing strand-specific RT-qPCR (Fig. 6) [28]. In cells infected with a non-irradiated virus suspension, both cRNA and mRNA were significantly lower than vRNA at 2 h post-infection (Supplemental fig. S2a). At 6 and 8 h post-infection, the three RNAs increased, and both vRNA and mRNA were significantly higher than cRNA levels (Supplemental fig. S2b). At 2 h post-infection, no difference was observed between both vRNA and cRNA levels of irradiated and non-irradiated virus suspensions (Fig. 6a and b), suggesting that UV-LED irradiation did not affect the virus incorporation into the host cells. All three UV-LED irradiations decreased vRNA, cRNA, and mRNA levels in host cells at both 6 and 8 h post-infection (Fig. 6). From these results, the viral inactivation effects of UVA-, UVB-, and UVC-LED irradiation might depend on inhibition of replication and transcription of vRNA in host cells.

3.6. Inactivation Effect of Irradiation of Different UV-LEDs on HPAI H5N1 Subtype

To observe the inactivation effect of UV-LEDs on HPAIs, we irradiated an HPAI H5N1 subtype (strain A/crow/Kyoto/53/2004) and compared FFUs between suspensions with and without irradiation. The fluences of UV-LEDs were fixed at 31.8 J/cm^2 (UVA-LED), 1.32 J/cm^2 (UVB-LED), and 0.055 J/cm^2 (UVC-LED), respectively, which were capable of decreasing the PFUs of H1N1 subtype 1000-fold ($\log_{10} = -3$), except UVA-LED (Fig. 2). In the irradiation experiment involving the H5N1 subtype, UVB-LED and UVC-LED decreased the FFUs > 10,000-fold, indicating that UVB- and UVC-LED irradiation had

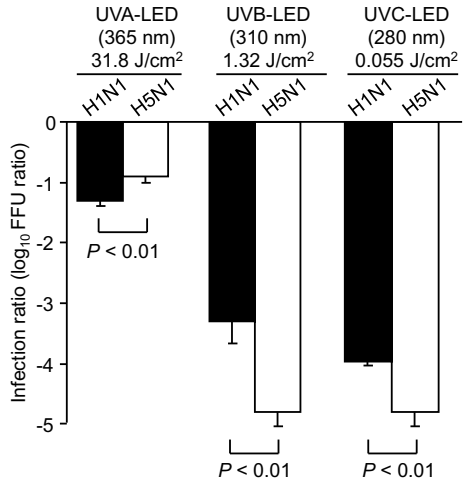

Fig. 7. Inactivation effects of UV-LED irradiation on H1N1 and H5N1 subtypes. Viral suspensions of different subtypes, H1N1 subtype (strain A/Puerto Rico/8/1934) and H5N1 subtype (strain A/crow/Kyoto/53/2004), were irradiated using different peak wavelength UV-LEDs and infected into MDCK cells. The fluences of UV-LEDs were fixed at 31.8 J/cm^2 (UVA-LED), 1.32 J/cm^2 (UVB-LED), and 0.055 J/cm^2 (UVC-LED). The viral inactivation effects of these irradiations were determined by infection ratio ($\log_{10}$), the ratio of focus-forming units (FFUs), as described in the Materials and Methods section. Values are shown as means ± SD (n = 3–4, n = number of independent replicates). $P < 0.01$ was considered significant.

high efficiencies for inactivation of the H5N1 subtype. These results suggest that the sensitivities to UV-LED irradiation differ among IAV subtypes (Fig. 7). However, the decrease in FFUs of H5N1 by UVA-LED irradiation was lower than H1N1 in this study, indicating that UVA-LED was not suitable for inactivation of HPAI viruses.

4. Discussion

In this study, we compared the viral inactivation effects of different peak wavelength UV-LEDs on IAV H1N1 subtype. UVA-LED irradiation could decrease 99% viral infectivity, but it displayed the lowest inactivation efficiency among the other UV-LED irradiations because it required the longest irradiating time and largest fluence (Fig. 2). We previously reported that the bactericidal effect of UVA-LED irradiation depended on inducing reactive oxygen species [21]. However Belanger et al. reported that UVA irradiation alone could not induce ROS in IAV H1N1 subtype and human immunodeficiency virus (HIV), but ROS induction could be achieved by photosensitization with aryl azide [28]. Additionally, Cui et al. reported that short-time irradiation of 365 nm UVA under black light could not inactivate IAV H9N2 subtype, but could be achieved using the photosensitizer titanium oxide [29]. Furthermore, irradiation of wavelengths > 610 nm with the photosensitizer monosubstituted zinc(II) phthalocyanine induced ROS and inactivated IAV H1N1 subtype and herpes simplex virus [30]. Unlike bacteria, viruses do not have cells and cannot grow independently. Delcanale et al. identified the localizations of some native photosensitizing molecules in bacterial cells [31]. These findings suggest that UVA irradiation to virions would not induce ROS and photosensitizers might be necessary to increase viral inactivation via ROS generation.

Low-pressure mercury UVC-lamps (254 nm) can inactivate viral and microbial pathogens by effecting genomic damage [8]. However, detailed mechanisms of virus inactivation by irradiation at other UV wavelengths, such as UVA, UVB, and near UVC remain unclear. It is well known that the absorption wavelength of DNA or RNA is approximately 260 nm and approximately 280 nm for protein. HA is a hemagglutination protein. It is the most abundant protein on the viral surface and binds to SA residues of cellular receptors to attach to the host cell surface [2]. Ogata N reported that chlorine dioxide decreased hemagglutination titer in IAV H1N1 subtype due to oxidation of the conserved tryptophan 153 residue in the receptor-binding site of HA protein [32]. Similar to the UV-LED irradiations in this study (Fig. 4), low-pressure mercury UV-lamps (254 nm) do not affect HA activity, as determined by measuring the hemagglutination titer (data not shown). This suggests that the viral inactivation effect of UV-LED irradiation does not depend on an alteration of HA protein activity and its oxidation. Furthermore, UV-LED irradiation did not affect vRNA levels in the host cells at 2 h post-infection (Fig. 6a). Therefore, UV-LED irradiation may not affect virus attachment and incorporation into the host cells. In our experiments measuring three RNA species using strand-specific RT-qPCR, UV-LED irradiation inhibited transcription and replication of viral RNA in the host cells (Fig. 6). In IAVs, viral ribonucleoprotein (vRNP) complexes, which consist of genome segments, three RNA polymerases, and nucleoprotein (NP), play critical roles in transcription and translation of viral RNAs. The 5′ and 3′ terminals of the vRNA are bound by a heterotrimeric RNA-dependent RNA polymerase, and the remainder of the vRNA associates with the NP. Following viral infection, the vRNPs are transported inside the host cell nucleus, where the RNA polymerases carry out both transcription of viral genes and replication of vRNA in the context of the vRNP [1]. UV-LED irradiations may induce some damage to vRNP complexes, but further in-depth experiments, such as measurement of vRNA damage in irradiated virions, are required.

We compared the viral inactivation effects of different UV-LEDs on different IAV subtypes H1N1 and HPAI H5N1. HPAI H5N1 was more effeiciently inactivated by UVB- and UVC-LED irradiation than H1N1 subtype (Fig. 7). However, the crucial factors responsible for the different IAV strain-specific sensitivities to UV irradiation remain unelucidated. Sasaki et al. reported that IAV H1N1 subtype had a higher resistance to pH decrease by β-propiolactone than H3N2, and the pH sensitivity was dependent on the susceptibility of viral M1 protein modification [33]. In our study, UV-LED irradiation did not alter the pH because the virus suspensions for the irradiations were diluted in a buffered solution, PBS (data not shown). The different host responses between H1N1 and HPAI viruses may be another factor contributing to the subtype sensitivities to UV irradiations. Sutejo et al. reported that growth of LPAI viruses in mammalian cells was lower than that of the H1N1 subtype, but growth in avian cells showed similar levels [34]. Therefore, further infection experiments involving avian cells are necessary to assess the inactivation effect of UV-LEDs on AIs.

In our study, both UVB- and UVC-LED irradiations demonstrated highly efficient inactivation of HPAI virus H5N1 (Fig. 7). Sutton et al. reported that two HPAI viruses, H5N1 and H7N1, were inactivated to similar levels by UVB-lamp irradiation [23], suggesting that the UV-LED irradiations were a useful inactivation method for other HPAI viruses. As the reports about the effect of UV-LED on other viruses, 280 nm UVC-LED inactivated coliphages under lower fluence than IAVs in this study [18,35]. However, larger fluence of 280 nm UVC-LED than IAVs was needed for inactivation to human adenovirus serotype 2 (HAdV2), a resistant pathogens to UV irradiation [20]. These suggest that the sensitivities against UV-LED irradiation are different among virus species and subtypes, and the other strategies of UV-LED irradiation are necessary for inactivating UV resistant subtypes. Our previous report showed that a combination of UVA-LED (365 nm) and UVC-lamp (254 nm) irradiation had a synergistic bactericidal effect on *Vibrio parahaemolyticus* depended on the suppression of the CPDs repairs such as recA- and lexA-mediated SOS responses. [36]. Our previous data was supported by Xiao Y et al. who reported that some synergistic inactivation effects on *E. coli* using combined 265/365 nm UV-LEDs [17]. However some reports showed that the combination of UVC- (265 and/or 280 nm) and UVB- (310 nm) LEDs had no synergistic on *E. coli* [14,18]. From these results, a combination of UVA-LED and deep UV-LED around 265 nm irradiation might be a good strategy to increase the efficiency of IAV inactivation. Our study should contribute to

preventing the spread of IAVs and HPAI viruses. Because the external quantum efficiencies of AlGaN-based UV-LEDs remain < 2%, the development of higher quantum efficiencies is necessary for the application to viral inactivation in the near future.

Supplementary data to this article can be found online at https://doi.org/10.1016/j.jphotobiol.2018.10.017.

Acknowledgements

This work was supported by JSPS KAKENHI, Japan Grant Numbers 15H05287, 15H05295, 15K09576, and 18H03040. This study was supported by Support Center for Advanced Medical Sciences, Tokushima University Graduate School of Biomedical Sciences, Japan.

References

[1] A.J. Te Velthuis, E. Fodor, Influenza virus RNA polymerase: Insights into the mechanisms of viral RNA synthesis, Nat. Rev. Microbiol. 14 (2016) 479–493.
[2] H. Memczak, D. Lauster, P. Kar, S. Di Lella, R. Volkmer, V. Knecht, A. Herrmann, E. Ehrentreich-Förster, F.F. Bier, W.F. Stöcklein, Anti-hemagglutinin antibody derived lead peptides for inhibitors of influenza virus binding, PLoS ONE 11 (2016) e0159074.
[3] R. Sawicka, P. Siedlecki, B. Kalenik, J.P. Radomski, V. Sączyńska, A. Porębska, B. Szewczyk, A. Sirko, A. Góra-Sochacka, Characterization of mAb6-9-1 monoclonal antibody against hemagglutinin of avian influenza virus H5N1 and its engineered derivative, single-chain variable fragment antibody, Acta Biochim. Pol. 64 (2017) 85–92.
[4] E. Dejesus, M. Costa-Hurtado, D. Smith, D.H. Lee, E. Spackman, D.R. Kapczynski, M.K. Torchetti, M.L. Killian, D.L. Suarez, D.E. Swayne, M.J. Pantin-Jackwood, Changes in adaptation of H5N2 highly pathogenic avian influenza H5 clade 2.3.4.4 viruses in chickens and mallards, Virology 499 (2016) 52–64.
[5] K. Sawabe, K. Hoshino, H. Isawa, T. Sasaki, K.S. Kim, T. Hayashi, Y. Tsuda, H. Kurahashi, M. Kobayashi, Blow flies were one of the possible candidates for transmission of highly pathogenic H5N1 avian influenza virus during the 2004 outbreaks in Japan, Influenza Res. Treat. 201 (2011) 652652.
[6] R. El-Shesheny, A. Mostafa, A. Kandeil, S.H. Mahmoud, O. Bagato, A. Naguib, S.E. Refaey, R.J. Webby, M.A. Ali, G. Kayali, Biological characterization of highly pathogenic avian influenza H5N1 viruses that infected humans in Egypt in 2014-2015, Arch. Virol. 62 (2017) 687–700.
[7] World Health Organization, Cumulative number of confirmed human cases for avian influenza A (H5N1) reported to WHO 2003–2016, (2016).
[8] W. Thanapongtharm, T.P. Van Boeckel, C. Biradar, X.M. Xiao, M. Gilbert, Rivers and flooded areas identified by medium-resolution remote sensing improve risk prediction of the highly pathogenic avian influenza H5N1 in Thailand, Geospat. Health 8 (2013) 193–201.
[9] Y. Yan, J.Y. Gu, Z.C. Yuan, X.Y. Chen, Z.K. Li, J. Lei, B.L. Hu, L.P. Yan, G. Xing, M. Liao, J.Y. Zhou, Genetic characterization of H9N2 avian influenza virus in plateau pikas in the Qinghai Lake region of China, Arch. Virol. 162 (2017) 1025–1029.
[10] J. Fawell, D. Robinson, R. Bull, L. Birnbaum, G. Boorman, B. Butterworth, P. Daniel, H. Galal-Gorchev, F. Hauchman, P. Julkunen, C. Klaassen, S. Krasner, J. Orme-Zavaleta, J. Reif, R. Tardiff, Disinfection by-products in drinking water: critical issues in health effects research, Environ. Health Perspect. 105 (1997) 108–109.
[11] D. Wang, J.R. Bolton, S.A. Andrews, R. Hofmann, Formation of disinfection by-products in the ultraviolet/chlorine advanced oxidation process, Sci. Total Environ. 518-519 (2015) 49–57.
[12] P.A. Ariya, M. Amyot, A. Dastoor, D. Deeds, A. Feinberg, G. Kos, A. Poulain, A. Ryjkov, K. Semeniuk, M. Subir, K. Toyota, Mercury physicochemical and biogeochemical transformation in the atmosphere and at atmospheric interfaces: a review and future directions, Chem. Rev. 115 (2015) 3760–3802.
[13] J.D. Park, W. Zheng, Human exposure and health effects of inorganic and elemental mercury, J. Prev. Med. Public Health 45 (2012) 344–352.
[14] K. Oguma, R. Kita, H. Sakai, M. Murakami, S. Takizawa, Application of UV light emitting diodes to batch and flow-through water disinfection systems, Desalination 328 (2013) 24–30.
[15] I. Delrue, P.L. Delputte, H.J. Nauwynck, Assessing the functionality of viral entry-associated domains of porcine reproductive and respiratory syndrome virus during inactivation procedures, a potential tool to optimize inactivated vaccines, Vet. Res. 40 (2009) 62.
[16] C. Bowker, A. Sain, M. Shatalov, J. Ducoste, Microbial UV fluence-response assessment using a novel UV-LED collimated beam system, Water Res. 45 (2011) 2011–2019.
[17] Y. Xiao, X.N. Chu, M. He, X.C. Liu, J.Y. Hu, Impact of UVA pre-radiation on UVC disinfection performance: Inactivation repair and mechanism study, Water Res. 141 (2018) 279–288.
[18] G.Q. Li, W.L. Wang, Z.Y. Huo, Y. Lu, H.Y. Hu, Comparison of UV-LED and low pressure UV for water disinfection: Photoreactivation and dark repair of Escherichia coli, Water Res. 126 (2017) 134–143.
[19] S. Rattanakul, K. Oguma, Inactivation kinetics and efficiencies of UV-LEDs against Pseudomonas aeruginosa, Legionella pneumophila, and surrogate microorganisms, Water Res. 130 (2018) 31–37.
[20] S.E. Beck, H. Ryu, L.A. Boczek, J.L. Cashdollar, K.M. Jeanis, J.S. Rosenblum, O.R. Lawal, K.G. Linden, Evaluating UV-C LED disinfection performance and investigating potential dual-wavelength synergy, Water Res. 109 (2017) 207–216.
[21] 21 A. Hamamoto, M. Mori, A. Takahashi, M. Nakano, N. Wakikawa, M. Akutagawa, T. Ikehara, Y. Nakaya, Y. Kinouchi, New water disinfection system using UVA light-emitting diodes, J. Appl. Microbiol. 103 (2007) 2291–2298.
[22] A. Hashimoto, K. Mawatari, Y. Kinouchi, M. Akutagawa, N. Ota, K. Nishimura, T. Hirata, A. Takahashi, Inactivation of MS2 phage and *Cryptosporidium parvum* oocysts using UV-A from high-intensity light-emitting diode for water disinfection, J. Water Environ. Tech. 11 (2013) 299–307.
[23] D. Sutton, E.W. Aldous, C.J. Warren, C.M. Fuller, D.J. Alexander, I.H. Brown, Inactivation of the infectivity of two highly pathogenic avian influenza viruses and a virulent Newcastle disease virus by ultraviolet radiation, Avian Pathol. 42 (2013) 566–568.
[24] D. Lénès, N. Deboosere, F. Ménard-Szczebara, J. Jossent, V. Alexandre, C. Machinal, M. Vialette, Assessment of the removal and inactivation of influenza viruses H5N1 and H1N1 by drinking water treatment, Water Res. 44 (2010) 2473–2486.
[25] T. Daidoji, Y. Watanabe, M.S. Ibrahim, M. Yasugi, H. Maruyama, T. Masuda, F. Arai, T. Ohba, A. Honda, K. Ikuta, T. Nakaya, Avian influenza virus infection of immortalized human respiratory epithelial cells depends upon a delicate balance between hemagglutinin acid stability and endosomal pH, J. Biol. Chem. 290 (2015) 10627–10642.
[26] J.G. Choi, Y.H. Jin, J.H. Kim, T.W. Oh, N.H. Yim, W.K. Cho, J.Y. Ma, *In vitro* antiviral activity of Psoraleae semen water extract against influenza a viruses, Front. Pharmacol. 7 (2016) 460.
[27] E. Kawakami, T. Watanabe, K. Fujii, H. Goto, S. Watanabe, T. Noda, Y. Kawaoka, Strand-specific real-time RT-PCR for distinguishing influenza vRNA, cRNA, and mRNA, J. Virol. Methods 173 (2011) 1–6.
[28] J.M. Belanger, Y. Raviv, M. Viard, U. Baxa, R. Blumenthal, Orthogonal inactivation of influenza and the creation of detergent resistant viral aggregates: towards a novel vaccine strategy, Virol. J. 9 (2012) 72.
[29] H. Cui, J. Jiang, W. Gu, C. Sun, D. Wu, T. Yang, G. Yang, Photocatalytic inactivation efficiency of anatase Nano-TiO(2) Sol on the H(9) N(2) avian influenza virus, Photochem. Photobiol. 86 (2010) 1135–1139.
[30] M.R. Ke, J.M. Eastel, K.L. Ngai, Y.Y. Cheung, P.K. Chan, M. Hui, D.K. Ng, P.C. Lo, Photodynamic inactivation of bacteria and viruses using two monosubstituted zinc (II) phthalocyanines, Eur. J. Med. Chem. 84 (2014) 278–283.
[31] P. Delcanale, F. Pennacchietti, G. Maestrini, B. Rodríguez-Amigo, P. Bianchini, A. Diaspro, A. Iagatti, B. Patrizi, P. Foggi, M. Agut, S. Nonell, S. Abbruzzetti, C. Viappiani, Subdiffraction localization of a nanostructured photosensitizer in bacterial cells, Sci. Rep. 5 (2015) 15564.
[32] N. Ogata, Inactivation of influenza virus haemagglutinin by chlorine dioxide: oxidation of the conserved tryptophan 153 residue in the receptor-binding site, J. Gen. Virol. 93 (2012) 2558–2563.
[33] Y. Sasaki, N. Yoshino, S. Sato, Y. Muraki, Analysis of the beta-propiolactone sensitivity and optimization of inactivation methods for human influenza H3N2 virus, J. Virol. Methods 235 (2016) 105–111.
[34] R. Sutejo, D.S. Yeo, M.Z. Myaing, C. Hui, J. Xia, D. Ko, P.C. Cheung, B.H. Tan, R.J. Sugrue, Activation of type I and III interferon signalling pathways occurs in lung epithelial cells infected with low pathogenic avian influenza viruses, PLoS ONE 7 (2012) e33732.
[35] D.K. Kim, S.J. Kim, D.H. Kang, Inactivation modeling of human enteric virus surrogates, MS2, Qβ, and ΦX174, in water using UVC-LEDs, a novel disinfecting system, Food Res. Int. 91 (2017) 115–123.
[36] M. Nakahashi, K. Mawatari, A. Hirata, M. Maetani, T. Shimohata, T. Uebanso, Y. Hamada, M. Akutagawa, Y. Kinouchi, A. Takahashi, Simultaneous irradiation with different wavelengths of ultraviolet light has synergistic bactericidal effect on *Vibrio parahaemolyticus*, Photochem. Photobiol. 90 (2014) 1397–1403.